ELSEVIER

Journal of Nuclear Materials 248 (1997) 386–391

journal of nuclear materials

Novel interferometers for femtosecond phase spectroscopy

Takayoshi Kobayashi *, Kazuhiko Misawa

Department of Physics, University of Tokyo, 7-3-1 Hongo, Bunkyo-ku, Tokyo 113, Japan

Abstract

Two novel interferometers, a frequency-domain Michelson interferometer (FDI) and a space-domain Sagnac interferometer (SI), are presented for the measurement of the difference phase spectra (DPS) with a femtosecond time resolution. Using these two interferometers, simultaneous measurement of time-resolved difference transmission spectra (DTS) and DPS of CS_2 is demonstrated over a full spectral region of femtosecond continuum. © 1997 Elsevier Science B.V.

1. Introduction

Interferometry is widely used to measure variations in the phase front of light among several optical methodologies. This technique has been applied to the measurements of dimensions such as length, shape, displacement, and surface roughness in the field of metrology. The minimum detection limit of such displacement measurements lies below nanometers.

Another important application of the interferometry is measurement of refractive index of materials. Two individual physical valuables describing light are phase and amplitude. The real and imaginary parts of the complex refractive index are related to the phase and amplitude of light in materials, respectively. Since optical detectors are basically used to measure the light intensity, i.e., the squared amplitude, absorbance, which is equivalent to the imaginary part of the refractive index, is easily measured. Phase change or difference is detected by the light intensity change or modulation in interferometry, and it can be used to measure change in the real part of the refractive index.

Femtosecond phase spectroscopy is important as well as absorption spectroscopy for studies of ultrafast phenomena in dispersive materials. The time dependence of the refractive-index change induced by optical excitation can be measured by means of time-resolved interferometry. One of the basic configurations in the interferometry is an amlitude-division interferometer [1–4]. A light beam is divided into two beams, which travel along different optical paths. One of the two is directed through a sample and is combined with the other after the sample to observe interference fringes.

Time-division interferometry (TDI) [5,6] is also used to measure the transient refractive-index change, where the probe and reference are temporally displaced but traveling collinearly in a single arm. The time delay of the excitation pulse with respect to the probe is set with a variable delay so that the excitation pulse passes through the sample after and before the arrival time of the reference and probe, respectively. In the presence of the excitation, only the probe pulse experiences the transient refractive index change. The phase change induced by the optical excitation can be measured from the phase difference between the interference fringes with and without the excitation. The advantage of the TDI is a higher visibility of the interference fringes, because both the reference and probe pulses transmit through the sample, and consequently, they have almost the same spectrum. In addition, the configuration is more stable against path length fluctuation, because the reference and probe pulses travel along a common path.

It is also important to measure the phase spectrum directly in the time-resolved spectroscopy by a single-shot experiment. However, most of the previous studies have been performed at single wavelengths of both the excitation and probe [1–5]. Since it was impossible to measure time-resolved phase spectrum before our studies using the frequency-domain interferometer, the Kramers–Kronig (K–K) relations had been used to obtain the spectral

* Corresponding author. Tel.: +86-3 3812 2111; fax: +81-3 3818 7812; e-mail: takakoba@phys.s.u-tokyo.ac.jp.

PII S0022-3115(97)00176-1

dispersion of the time-resolved refractive index change from the time-resolved absorbance change. The K–K relations have been found to be invalid in the time-resolved spectroscopy under some conditions [7]. Therefore, the real and imaginary parts of the complex refractive index changes should be measured directly and individually.

In the present paper, simultaneous measurement of the difference transmission and phase spectra is demonstrated by means of a frequency-domain Michelson interferometer and a space-domain Sagnac interferometer. These two interferometers accomplish the combination of the two optical methodologies, i.e., interferometry and spectroscopy. The frequency-domain interferometer was utilized for the first measurement of a femtosecond time-resolved phase spectrum as described in Section 3. In Section 4, femtosecond phase spectroscopy using one of the common-path interferometers, a Sagnac interferometer, is described.

2. Experimental

For the experiments of the frequency-domain interferometer (FDI), the amplified CPM pulses (620 nm, 60 fs, 2 μJ at 10 kHz) are divided into the pump and probe pulses. The probe is focused into an ethylene glycol jet to generate a white continuum. Fig. 1 shows the experimental setup for FDI. The continuum pulse is further divided into two in a Michelson interferometer for the reference and probe, and the two pulses are displaced temporally by a few hundreds of femtoseconds. Then they travel along a common path through a sample and are detected by a spectrometer with a multi-channel photodiode array.

The experiments of the Sagnac interferometer (SI) were performed with laser pulses (780 nm, 200 fs, 200 μJ at 1 kHz) from a Ti:sapphire regenerative amplifier (Clark-MXR, NJA-4/CPA-1000). The probe and reference pulses were divided from a white continuum generated by focusing the amplified pulses into CCl_4. Fig. 2 shows the

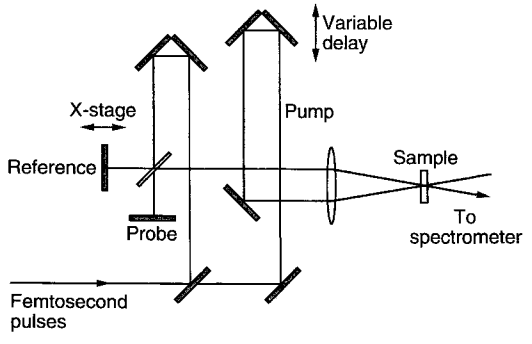

Fig. 1. Experimental setup of the frequency-domain interferometer.

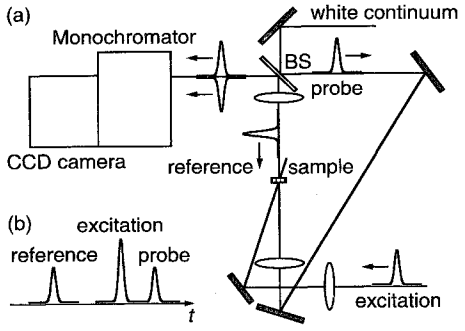

Fig. 2. (a) Experimental setup of the Sagnac interferometer, BS: beam splitter. (b) Time course of the excitation, reference, and probe pulses at the sample position.

diagram of the SI. The interferometer is composed of a chromium-coated beam splitter and two aluminum mirrors in a triangular configuration. A pair of confocal lenses are inserted in one side of the triangle. The sample was placed at the confocal position of these lenses. The output spatial fringes from the interferometer were detected using a digital CCD camera at each time delay between the excitation and probe, after dispersion with a monochromator.

The sample used in both measurements was CS_2 in a 1 mm thick quartz cell. The excitation for the measurement of time-resolved refractive index changes was also the amplified fundamental pulses of each laser system, which passed through a variable delay.

3. Frequency-domain interferometer (FDI)

3.1. Principle of FDI

The setup of FDI employs the time-division scheme for separating the reference from the probe. In the FDI [6], the temporal broadening of probe and reference pulses takes place in a monochromator due to the Fourier transform relation between spectral width and pulse duration. The broadened probe and reference pulses overlap with each other.

The principle of the femtosecond time-resolved phase spectroscopy by means of the FDI is based on the spectrometer which gives the Fourier transform of the incident light pulse. The probe and reference pulses are temporally displaced by T in the interferometer and transmitted through a medium. The Fourier amplitudes of the probe and reference fields are given by

$$E_{\mathrm{pr}}(\omega) = F\left[E_{\mathrm{pr}}(t)\right] = E(\omega-\omega_0)\exp\left(-\mathrm{i}n_{\mathrm{c}}(\omega)\omega d/c\right),$$

$$E_{\mathrm{ref}}(\omega) = E(\omega-\omega_0)\exp\left(-\mathrm{i}\omega T-\mathrm{i}n_{\mathrm{c}}(\omega)\omega d/c\right).$$

Here, ω_0 is a central angular frequency and $E(\omega)$ is generally a complex function, d is the thickness of the

medium, c is the light velocity in vacuum, and $n_c(\omega)$ is the complex refractive index of the medium defined by

$$n_c(\omega) = n(\omega) - ik(\omega).$$

The probe pulse undergoes a change in the complex refractive index, $\Delta n_c(\omega, \tau) = \Delta n(\omega, \tau) - i\Delta k(\omega, \tau)$, upon excitation such that

$$E_{pr}(\omega, \tau) = F\left[E_{pr}(t, \tau)\right] = E_{pr}(\omega)\exp(i\Delta\Phi(\omega, \tau) - \Delta K(\omega, \tau)),$$

where $\Delta\Phi \equiv -\Delta n\omega d/c$ and $\Delta K \equiv \Delta k\omega d/c$.

The interference signal without excitation measured with a spectrometer is expressed by

$$|E_{pr}(\omega) + E_{ref}(\omega)|^2 = |E_{pr}(\omega)|^2(2 + 2\cos\omega T)$$

and with excitation by

$$|E_{pr}(\omega, \tau) + E_{ref}(\omega)|^2 = |E_{pr}(\omega)|^2\{1 + \exp[-2\Delta K(\omega, \tau)] + 2\exp[-\Delta K(\omega, \tau)]\cos[\omega T - \Delta\Phi(\omega, \tau)]\}.$$

Comparing these two equations, $\Delta\Phi(\omega, \tau)$ and $\Delta K(\omega, \tau)$ can be simultaneously determined from the peak shifts and amplitude changes of the fringes, respectively, with a multi-channel spectrometer.

3.2. Results

Fig. 3(a) shows probe spectra with and without excitation and the difference transmission spectra, which were measured by blocking the reference beam [8]. Fig. 3(b) shows interference spectra with and without excitation and the difference phase spectra calculated from the fringe shift. This is the first measurement of the difference phase spectra (DPS) with a femtosecond time resolution [6–8].

The FDI has several advantages. First, the setup is obtained by adding only two more optical components, a beam splitter and a mirror, to the ordinary pump-probe setup. This is the simplest configuration of all the time-resolved interferometers developed so far. Since there is no need for overlapping the pulses temporally before the spectrometer, the configuration is much easier than the other setups. It is less sensitive to beam deflection because the path difference between the reference and probe consist only of the two very short arms of the Michelson interferometer. Hence, we could obtain the data with a high signal-to-noise ratio as shown in Fig. 3, even though a feedback technique for stabilization was not used. Second, optical alignment is much easier for overlapping the reference and probe either spatially or temporally in the setup. Readjusting the optical path difference between the reference and probe is not needed when the samples are exchanged. This FDI provided us a new possibility for time-resolved phase spectroscopy.

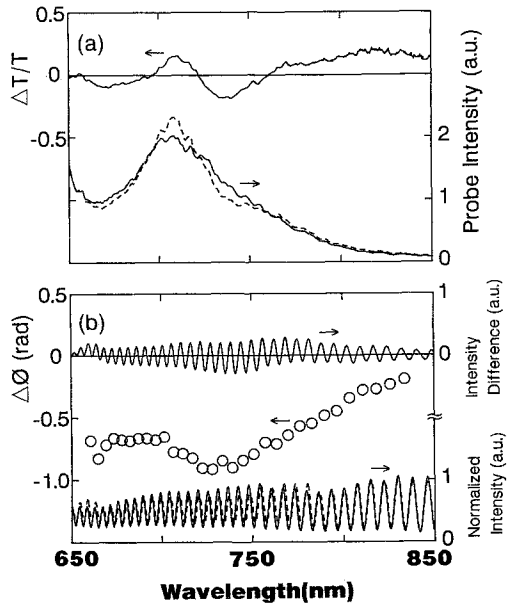

Fig. 3. Signals for CS_2 without delay-time correction obtained by the FDI. (a) DTS (upper solid curve) and probe spectra with (dashed) and without (lower solid). (b) DPS (open circles), interference spectra with (dashed) and without (lower solid) excitation, and the difference interference spectrum between them (upper solid).

To measure continuous DPS by FDI with the white-continuum light, the delay T between the reference and probe is necessary to be swept by the optical oscillation period. Otherwise, a space-division, not a time-division, configuration is preferred, where the reference and probe travel along different paths in a MZ interferometer to be spatially overlapped after the sample with time displacement T. In addition, the maximum time delay to obtain $\Delta\Phi(\omega, \tau)$ itself is limited by T. For $\tau > T$, the signal gives a difference between $\Delta\Phi(\omega, \tau - T)$ and $\Delta\Phi(\omega, \tau)$ because the reference is also influenced by the pump. Since the increase of T is limited by a system wavelength resolution, the maximum time delay is also limited. In the experiment, T was set at 310 fs. These features are improved in the femtosecond Sagnac interferometer described in the next chapter.

4. Sagnac interferometer (SI)

4.1. Principle of SI

To achieve high stability, one of the common-path interferometers, a Sagnac interferometer (SI), was utilized [9–11]. Furthermore, zeroth order interference of a white light can be automatically found in SI because of negligi-

ble optical path difference between the probe and reference pulses.

The essential point for the femtosecond SI is that the sample is not placed at the center [9–11]. The time course of the excitation, reference, and probe at the sample position is shown in Fig. 2(b). The counter-clockwise propagating reference pulse in the triangle passes through the sample first, and the clockwise probe pulse arrives at the sample almost after one round trip of the triangle. Since the probe and reference are temporally separated in the SI, SI is also used in a similar way to the TDI [5,6]. Even though the probe and reference pulses anti-collinearly propagate in the interferometer and the arrival time at the sample is displaced, they come out of the interferometer coincidentally. The maximum time delay was 2.2 ns determined by the time displacement between the reference and probe. This time displacement is much longer than for the FDI.

In the previous works using SI, transient change in either the refractive index [9,11] or absorbance [10] was measured at a fixed wavelength. However, it is important to measure simultaneously difference transmission and phase spectra using a multi-channel detector, as described above. The femtosecond SI in the present paper is most suited to the measurement of *continuous* dispersion of complex nonlinear optical susceptibility using femtosecond white continuum by a single shot [12]. One of the mirrors in the interferometer is slightly tilted to the vertical direction to measure nearly parallel spatial fringes due to interference of equal inclination between the probe and reference pulses. These recombined pulses are spectrally dispersed in a monochromator in the horizontal direction. Finally, the two-dimensional image with the vertical and horizontal axes of the optical path difference and wavelength, respectively, is detected with a two-dimensional detector. Hereafter, this two-dimensional image will be denoted as 'spectro-interferogram'.

Fig. 4(a)–(d) show the two-dimensional spectro-interferogram with time delays of the excitation of −2000, −300, 0, and 300 fs, respectively. The bright and dark lines represent the fringe peak and valley, respectively. The spectro-interferogram at −2000 fs (Fig. 4(a)) is equivalent to that without excitation. Fringe deformation due to the refractive index change in the sample is remarkably observed around the center wavelength in the image at −300, 0, and 300 fs (Fig. 4(b)–(d)).

4.2. Data analysis of SI

The vertical section of the spectro-interferogram corresponds to the interference fringe at a particular wavelength, which is called 'interferogram'. Fig. 5 shows the interferograms at 590 nm (a) without and (b) with excitation. The interferogram without excitation in (a) is also depicted in the same frame of (b) with excitation. Fringe phase shift is clearly observed in Fig. 5(b). The interfero-

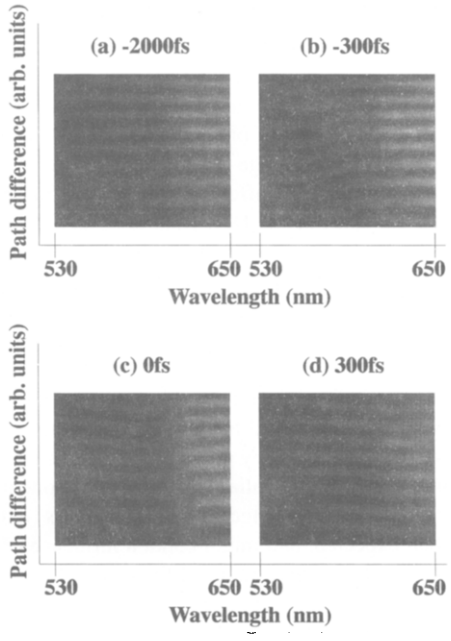

Fig. 4. Spectro-interferograms at time delays of (a) −2000, (b) −300, (c) 0 and (d) 300 fs detected with a CCD camera. The bright and dark lines represent the fringe peak and valley, respectively.

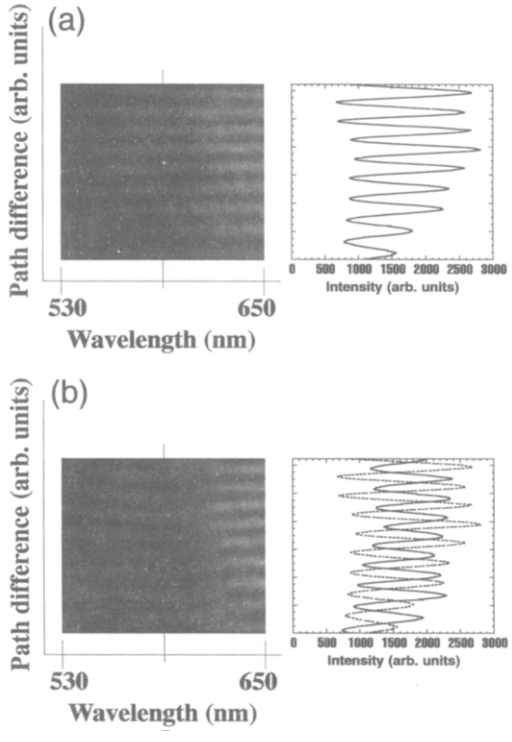

Fig. 5. Interferograms at 590 nm without (a) and with (b) excitation. The dashed curve in (b) represents the same interferogram in (a).

gram at every wavelength is a sine function in principle, but it is slightly distorted by imperfect condition such as wave-front distortion of the white continuum light. Hence the interferogram was Fourier-transformed to determine the amplitude and period of the interference fringe. From the phase shift of the fringe at each wavelength, we finally obtained time-resolved difference phase spectra shown in Fig. 6(a). The shift of the DPS peak is observed from blue to red, which is due to the spectral chirp in the probe white continuum.

If the imaginary part of the index change is not zero, the intensities of the probe and reference become unbalanced and as a result, the visibility of the interference fringe changes. The difference transmission spectrum can be individually determined from the spectro-interferograms as shown in Fig. 6(b). They are calculated from the Fourier amplitude of the main spatial-frequency component. However, transmissivity change obtained here is extremely larger than expected, and might contain influence of spatial beam deformation due to induced focusing. Accurate evaluation of transmissivity change is now being performed.

The time dependence of the phase change was fitted with a sum of two exponential functions $A_1 e^{-t/\tau_1} + A_2 e^{-t/\tau_2}$. Fig. 7 shows the time dependence of the phase change at 590 nm. The two time constants of exponential decay were determined to be $\tau_1 = 360 \pm 80$ fs and $\tau_2 = 1.7 \pm 0.6$ ps with the relative amplitude of $A_1 = 0.76$ and $A_2 = 0.24$. These values are close to the time constants previously reported [1]. This result shows that the time dependence of the phase change at particular wavelengths can be successfully measured. At different wavelengths the time-zero is observed to shift due to the chirp. By means of this principle, the group delay in the white continuum pulses can be measured in a similar way to Ref. [8]. Fig. 8 shows the $t - \lambda$ plot of the chirped continuum. The fitted curve represents a linear chirp induced by 22 mm thick BK7. This value is reasonable when all the optical components are considered including CCl_4 and CS_2.

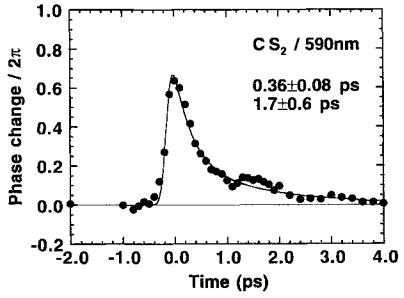

Fig. 7. Time dependence of the phase change in CS_2 at 590 nm. The solid line represents the decay profile fitted with a sum of two exponential functions. The decay time constants of these components are 360 ± 80 fs and 1.7 ± 0.6 ps.

4.3. Minimum detection limit of the phase change

A high-resolution CCD camera with 1000(H) × 1018(V) pixels was used for the SI experiments. The wavelength resolution on the camera was about 0.2 nm/pixel, but the resolution of the whole system was limited to ~ 1 nm by the slit width of the monochromator. The spectral range on the camera was about 200 nm (0.2 nm/pixel × 1000 pixels), but the effective area was limited to 530–650 nm with a center wavelength of 590 nm because of the strong stray light at the edges of the image.

The minimum detectable phase change is limited by the

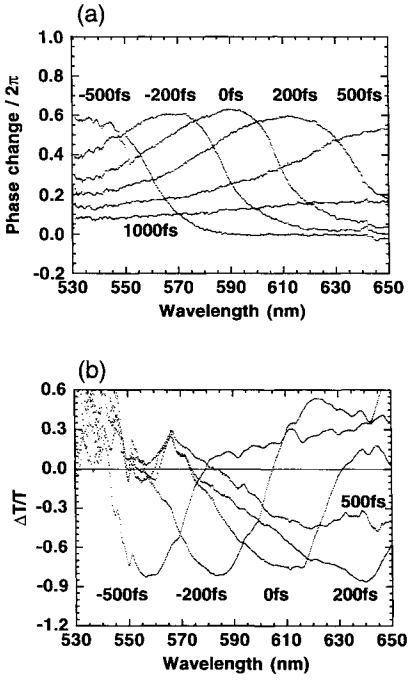

Fig. 6. Time-resolved DPS (a) and DTS (b) of CS_2 measured at several time delays. The spectral shift with the time delay is due to the chirp of the white continuum.

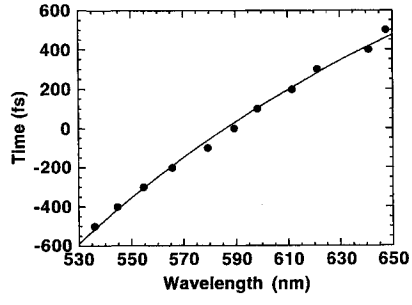

Fig. 8. $t - \lambda$ plot of the chirped continuum, which was obtained from the DPS in Fig. 6(a) by plotting the timedelays against the wavelengths at the peak of the DPS. The solid curve is the fitted with the Selmeier equation of BK7.

stability of the interferometer, the spatial resolution of the CCD camera, and error in determination of the sine function in the interferogram. In the present measurement, the frame-to-frame fluctuation was estimated to be $\sim \lambda/110$, which causes an error of the determined phase shift. The sensitivity in the phase difference of the whole system was evaluated from the standard deviation of the phase shift over interferogram to be $\sim \lambda/69$. Further improvement is expected by careful optimization of the spatial fringe. When the fringe spacing is larger, the precision of the fringe phase, which is determined by the spatial resolution of the camera, becomes higher. On the other hand, the error in determination of the phase becomes smaller, when the fringe spacing is smaller, consequently, the number of the fringe peak is larger. By adjustment of the equal inclination, the fringe spacing can be easily changed. In this way, we consider that the resolution of $\sim \lambda/200$ will be attained.

5. Conclusion

Novel femtosecond interferometers, a frequency-domain Michelson interferometer and a space-domain Sagnac interferometer, were developed for a single-shot measurement of DPS over a whole spectral region of white light continuum. The present methodology, interferometric spectroscopy, provides us full information of time-resolved complex nonlinear optical susceptibility. These femtosecond interferometers are useful for the single-shot measurements of the time-resolved difference transmission and phase spectra. Simultaneous determination of the real and imaginary parts of the complex susceptibility using the two interferometers was successfully demonstrated.

Acknowledgements

The authors would appreciate the experimental collaboration with Dr E. Tokunaga on FDI, and Mr A. Ueki and Mr H. Kanou on SI. This work is supported by Grant-in-Aid for Specially Promoted Research from the Ministry of Education, Science, and Culture (No. 05102002).

References

[1] J.M. Halbout, C.L. Tang, Appl. Phys. Lett. 40 (1982) 765.
[2] N. Finlayson, W.C. Banyai, C.T. Seaton, G.I. Stegeman, J. Opt. Soc. Am. B6 (1989) 675.
[3] D. Cotter, C.N. Ironside, B.J. Ainslie, H.P. Girdlestone, Opt. Lett. 14 (1989) 317.
[4] K. Minoshima, M. Taiji, T. Kobayashi, Opt. Lett. 16 (1991) 1683.
[5] M.J. LaGasse, K.K. Anderson, H.A. Haus, J.G. Fujimoto, Appl. Phys. Lett. 54 (1989) 2068.
[6] E. Tokunaga, A. Terasaki, T. Kobayashi, Opt. Lett. 17 (1992) 1131.
[7] E. Tokunaga, A. Terasaki, T. Kobayashi, Phys. Rev. A47 (1993) 4581.
[8] E. Tokunaga, A. Terasaki, T. Kobayashi, Opt. Lett. 18 (1993) 370.
[9] Y. Li, G. Eichmann, R.R. Alfano, Appl. Opt. 25 (1986) 209.
[10] R. Trebino, C.C. Hayden, Opt. Lett. 16 (1991) 493.
[11] M.C. Gabriel, J.N.A. Whitaker, C.W. Dirk, M.G. Kuzyk, M. Thakur, Opt. Lett. 16 (1991) 1334.
[12] K. Misawa, T. Kobayashi, Opt. Lett. 20 (1995) 1550.